

# Performance evaluation of the Inveon PET Scanner using GATE based on the NEMA NU-4 Standards

Lijun Lu, Nicolas Karakatsanis, *Member, IEEE*, Jianhua Ma, *Member, IEEE*, Zhaoying Bian, Yanjiang Han, Jing Tang, *Member, IEEE*, Arman Rahmim, *Senior Member, IEEE*, and Wufan Chen\*, *Senior Member, IEEE*

**Abstract**—The purpose of this study is to validate the application of GATE (Geant4 Application for Tomographic Emission) Monte Carlo simulation toolkit to model the performance characteristics of Siemens Inveon small animal PET system. GATE has been utilized to accurately create a complete PET imaging system model, including system geometry, physics process, signal processing and time-dependent effects. The GATE output data were histogrammed into 3D sinograms and subsequently processed by the Software of Tomography Reconstruction (STIR) to reconstruct 3D PET images. The simulation results were validated against experimental data in accordance with the NEMA NU-4 2008 protocol for standardized evaluation of spatial resolution, sensitivity, scatter fraction (SF) and noise equivalent counting rate (NECR) of a preclinical PET system. An agreement of less than 3% was obtained between the spatial resolution of the simulated and experimental results. The simulated peak NECR of mouse-size phantom agreed with the experimental result, while for the rat-size phantom simulated value was higher than experimental result. The simulated and experimental SFs of mouse- and rat- size phantom both reach an agreement of less than 2%. Therefore, it has been shown the feasibility of our GATE model to accurately simulate, within certain limits, all major performance characteristics of Inveon PET system. In future, the validated model can be utilized to validate, assess and further develop reconstruction algorithms and PET acquisition protocols.

## I. INTRODUCTION

POSITRON emission tomography (PET), a non-invasive molecular imaging technique, has been widely used for quantification of physiological and biochemical process in preclinical and clinical research [1]. The accuracy of quantitative studies depends on the quality of the acquired dynamic PET images [2]-[3]. However, the reconstructed images are

Manuscript received November 15, 2013. This work was supported by the 973 Program of China under Grant No. 2010CB732504, the U.S. National Institute of Health under grant 1S10RR023623, the U.S. National Science Foundation under grant ECCS-1228091, the Specialized Research Fund for the Doctoral Program of Higher Education under grant 20134433120017, and the National Natural Science Foundation of China under grants 81000613, 81101046 and 11205081.

L. Lu (e-mail: ljlubme@gmail.com), J. Ma (e-mail: jhma75@gmail.com), Z. Bian (e-mail: zybian86@gmail.com), and W. Chen\* (e-mail: chenwf@fimmu.com) are with the School of Biomedical Engineering, Southern Medical University, Guangzhou, Guangdong, China.

Y. Han (e-mail:riverhanyj@gmail.com) is with the Department of Nuclear Medicine, Nanfang Hospital, Southern Medical University, Guangzhou, Guangdong, China.

N. Karakatsanis (e-mail:nicolas.karakatsanis@gmail.com) and A. Rahmim (e-mail: arahmim1@jhmi.edu) are with the Department of Radiology, Johns Hopkins University, Baltimore, MD, USA. A. Rahmim is also with the Department of Electrical & Computer Engineering, Johns Hopkins University, Baltimore, MD, USA.

J. Tang (e-mail:jtang@oakland.edu) is with the Department of Electrical & Computer Engineering, Oakland University, Rochester, MI, USA.

commonly affected by scattered and random events as well as dead time and attenuation effects impairing the statistical quality of PET projection data.

The simulation of a PET system using Monte Carlo (MC) algorithms could define an accurate model for the real PET scanner enabling acquisition of realistic simulated data that, in practice, cannot be measured experimentally. Such a model can be used for the optimization of the system geometry, the acquisition protocol, the reconstruction algorithm as well as for enhanced image quantification [4]. Geant4 Application for Tomographic Emission (GATE) is an MC simulation platform based on GEANT4 core libraries, specifically designed to provide realistic models of complete PET/SPECT imaging systems through a user-friendly macro-command interface [5]. The Inveon dedicated PET scanner is the latest generation of commercial tomographs from Siemens Preclinical Solutions, Inc.[6]. The aim of this study is to evaluate the performance characteristics of the Inveon PET scanner using a validated GATE model. GATE version 6.1 is employed for the modeling while system performance evaluation is based on National Electrical Manufactures Association (NEMA) NU-4 standards, as it provides a standardized methodology for small animal PET performance evaluation [7]. The simulated projection data will be used to optimize reconstruction and enhance quantification of the images as reported in [8].

## II. METHODS AND MATERIALS

### A. Description of system

The Inveon PET system is a lutetium oxyorthosilicate (LSO)-based, high-sensitivity, high-resolution preclinical PET scanner(Fig.1). The system has been installed at the Nanfang Hospital of Southern Medical University at Guangzhou, Guangdong. It consists of 64 detector blocks arranged in 4 contiguous rings. Each detector block has a  $20 \times 20$  LSO crystal array configuration. Each crystal element is 10.0 mm long and has a cross-sectional area of  $1.51 \times 1.51$  mm. The crystal pitch is 1.59 mm in both axial and transverse directions. The crystal ring diameter is 16.1 mm while the transaxial and axial FOV are 10.0 mm and 12.7 mm, respectively.

GATE is a simulation platform designed to utilize the underlying well-validated physics components of Geant4. We selected to incorporate into our GATE simulation the low energy Geant4 models for the Compton, Rayleigh and photoelectric photon interactions.

Another interesting feature of GATE is the ability to simulate the conversion of photon interactions into digital counts in

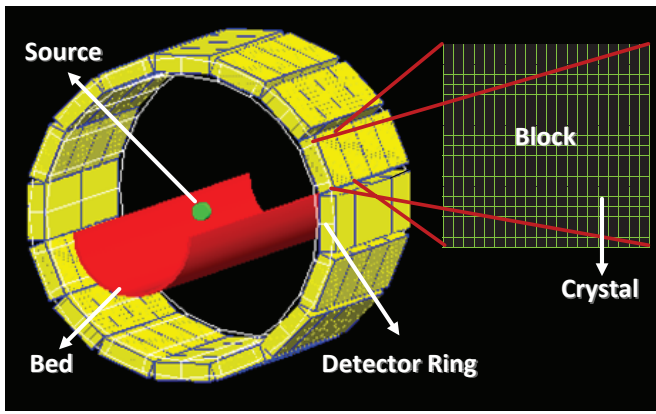


Fig. 1. Graphical representation of the geometry of the Inveon PET system as visualized by GATE. The LSO layer is depicted with yellow color.

an attempt to model the detector and electronic responses of a real scanner. The energy resolution of the 511 keV photopeak was set to 14.6% [6]. We applied a paralyzable approximate dead-time model in order to simulate the dead time both at singles and the coincidences level of the signal processor chain of the scanner. The dead time is set to 300 ns at the singles and 500 ns at the coincidence level.

### B. Spatial resolution

In accordance with the NEMA NU-4 2008 standards, we simulated a spherical  $^{22}\text{Na}$  point source with a nominal size (0.3 mm) to measure the spatial resolution. The activity of the source was 198kBq. The energy window was set to 350-625 keV and the coincidences time window (CTW) was 3.432 ns. The source was positioned at 2 axial positions (i.e. at the center and at one fourth (31.75) of the axial FOV distance) and the counts value is about 7 million.

The 3-dimensional (3D) sinograms were sorted into 2-dimensional (2D) sinograms by Fourier rebinning (FORE). Subsequently, the images were reconstructed using an analytic 2D filtered backprojection (FBP), with a ramp filter cut off at the Nyquist frequency. A zoom factor was selected to achieve a 0.39-mm-pixel in-plane resolution. The axial plane separation was 0.796 mm. The dimension of the reconstructed image is  $256 \times 256 \times 159$ .

### C. Sensitivity

An  $^{18}\text{F}$  point source was used to measure the absolute sensitivity of the system for different energy window settings. The  $^{18}\text{F}$  source was positioned at the center of the FOV and scanned for 5 mins. The CTW and dead time were set to 3.42ns and 500ns respectively. Two classes of energy windows were examined: a) one with a fixed 350 keV low-level discriminator (LLD) and a set of upper-level discriminators (ULDs) of 600, 625, 650, 700 keV respectively and b) the other with a fixed 625 keV ULD and LLDs of 300, 350, 400, 450 respectively.

Furthermore, to provide a sensitivity illustration over the complete FOV, we used a transaxial step size of 1 mm for the range of -5 to 5 mm and 5 mm for the range of 5-45 mm. The axial step size was 1 mm for the range of -5 to 5 mm and 5

mm elsewhere. For each position of the point source, the scan time was 5 seconds and the energy windows were 350-625keV.

### D. Scatter Fraction and Counting-Rate Performance

Scatter fraction and counting-rate performance were measured using 2 different cylindrical phantoms of high density polyethylene to model the geometries of a mouse and a rat. The design of the phantoms conformed to the NEMA NU-4 standards. The mouse-like phantom was a 70 mm long solid cylinder with a 25 mm diameter. A cylindrical hole (diameter, 3.2 mm) was drilled parallel to the central axis, at a radial distance of 10 mm. The rat like phantom was also cylindrical but with larger dimensions (length 150 mm; diameter 50 mm). An  $^{18}\text{F}$  source with a variable total activity from 10 MBq to 500MBq was utilized for both mouse- and rat- size phantom, respectively.

The scatter fraction was calculated by equation (1):

$$SF = \frac{R_s}{R_s + R_t} \quad (1)$$

While the corresponding noise equivalent counting rate (NECR) was given by equation (2):

$$NECR = \frac{R_t^2}{R_t + R_s + 2R_r} \quad (2)$$

where  $R_s$ ,  $R_t$ ,  $R_r$  are the scatter, true, and random counting rates, respectively.

## III. RESULTS

### A. Spatial Resolution

Table I shows the spatial resolution in FWHM of the 2D FBP reconstructed point-source images in the radial, tangential, and axial direction for 2 axial positions. At the center of the FOV, the image resolutions in the transverse planes were about 1.8 mm FWHM.

TABLE I  
TABLE I. SPATIAL RESOLUTION FOR TWO DIFFERENT AXIAL POSITION (THE CENTER OF THE AXIAL FOV AND ONE FOURTH (31.75) OF THE AXIAL FOV)

	Radial	Tangential	Axial	(mm)
Axial center	1.83	1.75	1.88	
1/4 axial FOV	1.92	1.95	2.01	

### B. Sensitivity

Table II comparatively presents the simulated and experimental (reported in [6]) absolute sensitivity for different energy windows. It can be observed that the absolute sensitivity is dropped to 5.93% when the LLD reaches 450keV.

Fig.2 presents the simulated absolute sensitivity for complete FOV of the Inveon scanner. We can note that the value of the absolute sensitivity is maximal at the center of the FOV. Also this result is similar to the experimental result reported in [9]. This may be useful for optimizing experiments by scanning more than 1 animal at the same time.

TABLE II

TABLE II. COMPARISON BETWEEN THE SIMULATED AND EXPERIMENTAL ABSOLUTE SENSITIVITY FOR DIFFERENT ENERGY WINDOWS SETTINGS.

Energy window	Experimental results	Simulated results
350-600	6.64%	6.79%
350-625	6.72%	6.82%
350-650	6.74%	6.83%
350-700	6.85%	6.86%
350-625	7.86%	7.63%
350-625	6.72%	6.82%
400-625	5.95%	6.52%
450-625	4.19%	5.79%

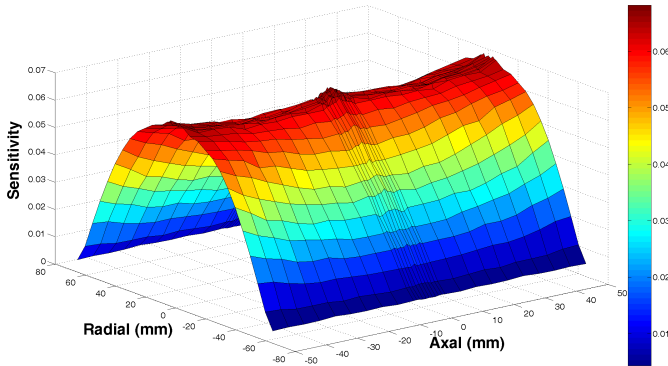


Fig. 2. Simulated sensitivity for complete FOV of the Inveon scanner.

### C. Scatter Fraction and Counting Rate Performance

Table III lists the simulated and experimental scatter fraction (reported in [6]) for the mouse- and rat- size phantom, respectively. The simulated value is a little higher than the value determined experimentally. Fig.3 shows the plots of simulated NECR as a function of total activity for mouse- and rat-sized phantoms. It can be observed that the NECR curve reaches the peak value, when the total activity is approximately 150 MBq. Table 4 lists the simulated and experimental NECR peak value (reported in [6]) for mouse- and rat- size phantom, respectively. The results indicate a good agreement between our simulated and experimental NECR peak value for mouse-size phantom. However, for the rat-size phantom, simulated peak NECR is higher.

TABLE III

TABLE III. COMPARISON OF THE INTRINSIC SCATTER FRACTION SIMULATED AND EXPERIMENTAL VALUES FOR BOTH MOUSE- AND RAT-SIZE PHANTOM.

SF	Mouse phantom	Rat phantom
Experimental results	7.8%	17.2%
Simulated results	9.7%	18.8%

## IV. CONCLUSION

In this study it has been shown that modeling of a commercial high-end PET preclinical system is feasible with

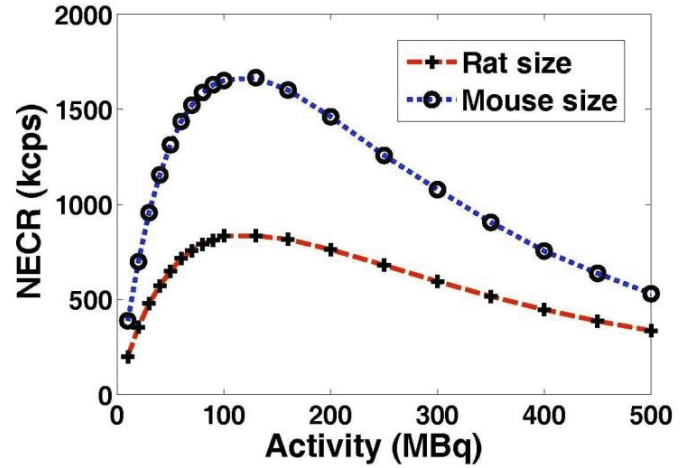


Fig. 3. Plots of simulated NECR as a function of total activity for mouse- and rat-sized phantoms.

TABLE IV

TABLE IV. COMPARISON OF THE PEAK NECRS SIMULATED AND EXPERIMENTAL VALUES FOR BOTH MOUSE- AND RAT-SIZED PHANTOM.

Peak NECR	Mouse phantom	Rat phantom
Experimental results	1670	590
Simulated results	1667	830

GATE by validating simulation against experimental results. Subsequently the validated GATE model was employed to evaluate the performance of a real PET system based on NEMA NU-4 standards. The results demonstrated the ability of the standard performance characteristics of the Siemens Inveon small animal PET system. The constructed model will be utilized in future to validate, assess and advance reconstruction algorithms and acquisition protocols of the Inveon PET system.

## V. ACKNOWLEDGMENTS

The authors wish to thank Profs. Uwe Pietrzyk and Michaela Gaens for offering the Radioactive decay patches for GATE V6.1.

## REFERENCES

- [1] A. Rahmim and H. Zaidi, PET versus SPECT: strengths, limitations and challenges, *Nucl. Med. Com.*, vol. 29, pp. 193-207, 2008
- [2] L. Lu, N. A. Karakatsanis, J. Tang, W. Chen, and A. Rahmim, 3.5D dynamic PET image reconstruction incorporating kinetics-based clusters, *Phys. Med. Biol.*, vol. 57, pp. 5035-5055, 2012.
- [3] A. Rahmim, Y. Zhou, J. Tang, L. Lu, V. Sossi, and D. F. Wong, D. F., Direct 4D parametric imaging for linearized models of reversibly binding PET tracers using generalized AB-EM reconstruction, *Phys. Med. Biol.*, vol. 57, pp. 733-755, 2012.
- [4] I. Buvat, and I. Castiglioni., Monte Carlo simulations in PET and SPECT, *Q. J. Nucl. Med.*, vol. 46, pp. 48-61, 2006.
- [5] Jan S., et al., GATE: a simulation toolkit for PET and SPECT, *Phys. Med. Biol.*, vol. 49: pp. 4543-4561, 2004.
- [6] Q. Bao, D. Newport, M. Chen, D. B. Stout, and F. A. Chatzioannou, Performance evaluation of the Inveon Dedicated PET preclinical tomograph based on the NEMA NU-4 Standards, *J. Nucl. Med.*, vol. 50: pp. 401-408, 2009.

- [7] National Electrical Manufacturers Association (NEMA), Performance Measurements for Small Animal Positron Emission Tomographs (PETs). NEMA Standards Publication NU 4-2008, *Roslyn, VA: NEMA*; 2008.
- [8] N. A. Karakatsanis, M. A. Lodge, A. K. Tahari, Y. Zhou, R. L. Wahl, and A. Rahmim, Dynamic whole-body PET parametric imaging: I. Concept, acquisition protocol optimization and clinical application, *Phys. Med. Biol.*, vol. 58, pp. 7391-7418, 2013.
- [9] P. E. Visser, A. J. Disselhorst, M. Brom, P. Laverman, M. Gotthardt, J. W. Oyen, and C. O. Boerman, Spatial resolution and sensitivity of the Inveon small-animal PET scanner, *J. Nucl. Med.*, vol. 50: pp. 139-147, 2009.